

# Nitrogen Implantation Into Amorphous Carbon Films: SIMS and Positron Annihilation Analyses

F. L. Freire Jr. and D. F. Franceschini

*Departamento de Física, Pontifícia Universidade Católica do Rio de Janeiro,  
22453-970, Rio de Janeiro, RJ, Brazil*

C. A. Achete

*Programa de Engenharia Metalúrgica e de Materiais, COPPE, UFRJ  
21915-970, Rio de Janeiro, RJ, Brazil*

I. J. R. Baumvol

*Instituto de Física, Universidade Federal do Rio Grande do Sul  
91500-970, Porto Alegre, RS, Brazil*

R. S. Brusa and G. Mariotto

*Dipartimento di Fisica, Università di Trento,  
38050, Povo, TN, Italy*

R. Canteri

*Divisione Materiali Innovativi, Centro Materiali e Biofisica Medical-ITC  
38050, Povo, TN, Italy*

Received July 21, 1995

Hard amorphous hydrogenated carbon films deposited by self-bias glow discharge were implanted at room temperature with 70 keV-nitrogen ions at fluences between  $2.0$  and  $9.0 \times 10^{16}$  N/cm<sup>2</sup>. The implantation energy was chosen so that the projected range plus range straggling ( $R_p + \Delta R_p$ ) was smaller than the film thickness. The implanted samples were analyzed by Raman scattering, Secondary ion mass spectrometry (SIMS) and positron annihilation spectroscopy, using the Doppler broadening technique with the determination of the shape parameter ( $S$  parameter). Depth profiles of implanted species agree well with the predictions of the Monte Carlo code, Transport of Ions in Matter (TRIM-90). For samples implanted with  $2 \times 10^{16}$  N/cm<sup>2</sup> the  $S$  parameter follows the vacancies depth profile predicted by the simulation. For higher fluences we observed a reduction in the measured value of  $S$ . The first result was interpreted as being due to the point defects generated during the ion stopping, whereas the PAS results for higher fluences were due to the structural modifications (increase of disorder and of the number, or size, of the graphitic domains) induced in the carbon films by the incident ions combined with the point defects generated by the atomic collisions.

## I. Introduction

Amorphous hydrogenated carbon films (a-C:H) have been the focus of considerable research efforts due to their electrical, mechanical and chemical properties<sup>[1,2]</sup>. Up to now, the studies on a-C:H films were mostly attempted to characterize, modify and optimize their structure and properties under a wide range of deposition parameters. In the last few years, the study of dopant incorporation into a-C:H films has re-

ceived special attention. The introduction of dopants into a-C:H films can, in principle, be obtained by either incorporation during film growth, *i.e.* growing the film in the presence of dopant atoms, or by post-growth implantation of dopants ions. Concerning nitrogen doping, the use of dopant-containing gases during the film deposition has been successfully employed to produce intentionally doped films by Plasma-Enhanced Chemical Vapor Deposition (PECVD)<sup>[3,4]</sup>. Ion implantation is scarcely used to dope a-C:H films. In fact, structural

modifications and hydrogen loss have a dominant effect on the electrical and optical properties of the implanted material<sup>[5–7]</sup>. Some attempts to dope a-C:H films with nitrogen by ion implantation do not show any encouraging indication of efficient chemical doping<sup>[5,7]</sup>. The main observed modifications, hydrogen loss and surface graphitization, were correlated with the total deposited energy by incident atoms in either elastic and inelastic collisions<sup>[8–10]</sup>.

On the other side, positron annihilation spectroscopy is one of the most sensitive techniques for the analysis of point defects in crystalline semiconductors<sup>[11]</sup>. However, until now only few studies on disordered carbon materials have been reported in the literature<sup>[12–15]</sup> and the interpretation of positron annihilation results is not well established as for crystalline materials. Efforts in that direction are still in the beginning.

In this paper, we report results on the investigation of depth distribution of ion-induced defects in nitrogen implanted a-C:H films by using positron annihilation spectroscopy (PAS), in order to gain some insights on the mechanisms of ion beam induced modifications and their influence on the positron annihilation mechanisms. To interpret PAS data, we have taken into account both Monte Carlo simulation results for the transport of ions in matter (TRIM-90)<sup>[16]</sup> and structural modifications, illustrated by Raman scattering results. SIMS depth profiles are also presented.

## II. Experimental procedures

a-C:H films (typically 350 nm thick) were deposited onto p-type Si (100) substrates mounted over a water-cooled stainless steel cathode of a Varian r.f. (13.56 MHz)-diode sputtering system. They were obtained by plasma decomposition of methane at a total pressure of 8 Pa and self-bias voltage  $V_b$ , of -370 V. Their chemical composition was: 86.1 atom % of C and 13.9 atom % of H (density = 0.21 g-at./cm<sup>3</sup>). After deposition, the samples were implanted at room temperature with 70 keV nitrogen ions at fluences between 2 and  $9 \times 10^{16}$  N/cm<sup>2</sup>. This incident energy was chosen so that the projected range plus range straggling of implanted ions ( $R_p + \Delta R_p \cong 150$  nm) falls within the film thickness, as calculated by a Monte Carlo-based code (TRIM-90).

The positron annihilation measurements were carried out using a variable-energy beam, supplemented by a 74 MBq  $\beta^+$  source of Na<sup>22</sup>. The energetic positrons were moderated by a 4  $\mu$ m thick W foil. The energy of the monoenergetic positron beam was varied from 0.2 to 30 keV. The 511 keV annihilation gamma was detected by a high-purity Ge detector (energy resolution of 1.8 keV at 1.33 MeV) with software stabilization. Details of the experimental apparatus are described elsewhere<sup>[17]</sup>. The Doppler-broadened annihilation gamma line carries information of the momentum of the electron-positron annihilation pair. A narrowing of the lines means that positrons are mainly annihilating with electrons with slow momentum, *i.e.* electrons in open volumes. The shape parameter  $S$  was used to characterize the annihilation gamma line. It is defined as the ratio between the counts in a central region of the annihilation line and the total number of the counts in the line. Of course, a narrowing of the line corresponds to an increase of the  $S$  parameter.

In order to determine the depth profile of implanted species and possible compositional modifications induced by the ion irradiation, SIMS analyses were performed. High mass-resolution depth profiles of positive ions were determined by using a CAMECA IMS-4f ion microprobe, with 20 nA-Cs<sup>+</sup> as the primary beam at an energy of 5.5 keV. The yields of molecular ions  $Cs_2X^+$  ( $X$  is the mass of each profiled species: hydrogen, carbon, nitrogen, oxygen and silicon) were recorded as a function of the sputtering time. The secondary-ion current was electronically gathered to 25% of the 100  $\mu$ m<sup>2</sup> rastered area to minimize crater edge effects. The conversion from sputtering time to depth was made by measuring both the thickness of the a-C:H films and the depth of the sputtered crater using a stylus profilometer.

Raman measurements were performed at room temperature in a backscattering configuration using a 488 nm argon laser beam at a power of 250 mW

## III. Results

The more representative SIMS profiles are reported in Fig. 1. The data presented in Fig. 1 a are plotted as a function of the sputtering time, while in Fig. 1b and Fig. 1c the data are plotted as a function of the depth. All samples have nearly same thickness. Fig. 1a

presents the results obtained from an as-deposited film, that is essentially uniform in composition, apart from a thin SiO<sub>2</sub> layer at the film/substrate interface. For simplicity, oxygen profiles are not shown in the other figures, as they are quite similar to the one presented in Fig. 1a. Nitrogen depth profiles obtained from implanted samples have a gaussian shape, slightly asymmetric, as expected for normal implantation depth profiles. The experimental value for the projected range,  $R_p=110$  nm, and the range straggling,  $\Delta R_p=25$  nm, are in good agreement with the values obtained using the TRIM-90 code, 127 nm and 25 nm, respectively. SIMS results are also in nice agreement with previous experiments using nuclear techniques<sup>[9,18]</sup>. In fact, 3.5 MeV-He backscattering spectrometry was used for profiling nitrogen in a-C:H films implanted with higher fluences ( $6 - 20 \times 10^{16}$  N/cm<sup>2</sup>) than those studied in the present work. In this previous work, the intensity of the nitrogen signal compared with the signal from the Si substrate is strong enough to permit the determination of the depth profiles with reasonable accuracy. The  $R_p$  (110 nm) and  $\Delta R_p$  (40 nm) values determined from the 3.5 MeV-He backscattering experiments are in good agreement with the present SIMS results. The SIMS technique, due to its higher mass resolution and sensitivity, permits the determination of nitrogen depth-profiles even for fluences as low as  $2 \times 10^{16}$  N/cm<sup>2</sup>.

Nitrogen implantation into a-C:H films induced hydrogen loss only for ion fluences higher than  $2 \times 10^{16}$  N/cm<sup>2</sup>. In fact, the hydrogen profile obtained from films implanted with the lowest fluence is identical to that measured from an as-deposited film (Fig. 1b). SIMS profiles show that hydrogen depletion occurs only at a near-surface layer,  $R_p + \Delta R_p$  thick, and increases with the ion fluence (Fig. 1c). Previous results obtained using elastic recoil detection analysis are quite similar<sup>[8,9,18]</sup>.

Fig. 2 presents PAS-Doppler broadening technique results. The  $S$  parameters obtained for samples implanted with several fluences of nitrogen are reported as a function of the mean implantation depth of positrons, which was calculated through the following relation:

$$x = A(E^n)/\rho \quad (1)$$

where  $A = 3.46 \text{ Kg}(\text{cm}^2 \text{ keV}^{1.55})$ ,  $n = 1.55$  according

to Ref. 14,  $\rho$  is the density expressed in g/cm<sup>3</sup> and  $E$  is the energy in keV.

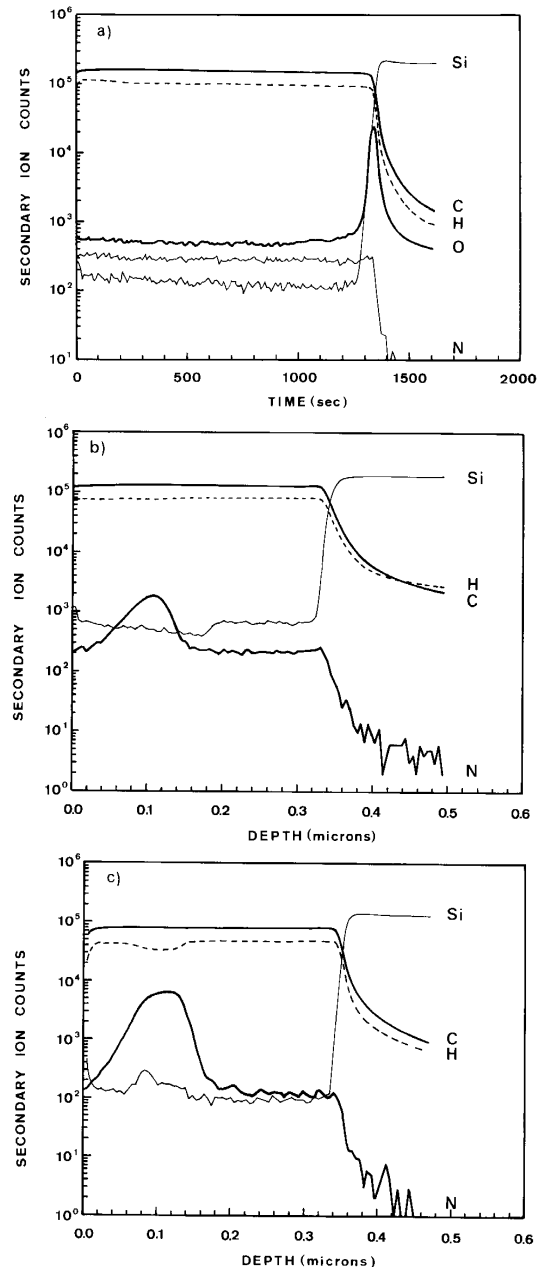


Figure 1. SIMS depth-profiles obtained from: (a) the as-deposited film (results presented as a function of the sputtering time); (b) a-C:H film implanted with  $2 \times 10^{16}$  70 keV-N/cm<sup>2</sup> and (c) a-C:H film implanted with  $6 \times 10^{16}$  70 keV-N/cm<sup>2</sup>.

In Fig. 2 the  $S$  parameters determined for the as-deposited and implanted films are shown.  $S$  was normalized to the value obtained at the Si substrate, *i.e.*, to a value that is reached in all samples for positron energies higher than 20 keV. In the unimplanted a-C:H sample,  $S$  remains constant throughout the film, starts to increase near the interface and finally reaches the

value of Si. The constancy of  $S$  means that the film is homogeneous and that the voids or open-volume structures have a constant distribution through the film.

The situation is completely different for the implanted samples. In fact, for the a-C:H film implanted with  $2 \times 10^{16}$  N/cm<sup>2</sup>, the  $S$  parameter presents a maximum centered at nearly 55 nm, decreases down to the characteristic value of an unimplanted film and then, at a depth close to that corresponding to the interface position, starts to increase. Samples implanted with higher fluences present similar depth profiles for the parameter  $S$ . They also present a flat shape with a maximum close to 55 nm, but the  $S$  value is systematically lower than the one obtained for the film implanted with the lowest fluence. For all implanted films there is a deepest layer, just beneath the interface, where  $S$  is equal to that measured in the as-deposited film. This result agrees with other techniques which have shown that ion beam induced modifications are confined in a surface layer,  $R_p + \Delta R_p$  thick<sup>[8-10]</sup>.

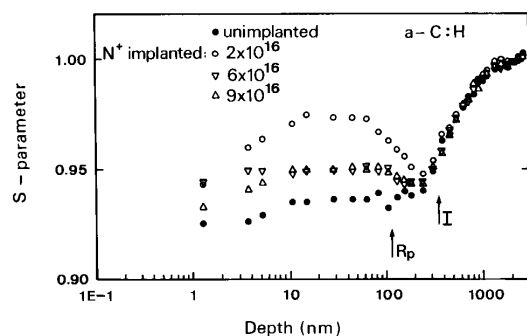


Figure 2.  $S$  parameter as a function of depth for a-C:H films implanted with nitrogen fluences between  $2$  and  $9 \times 10^{16}$  N/cm<sup>2</sup>. The arrows indicate the a-C:H/Si interface (I) and the experimental  $R_p$  position.

Raman spectra of the as-deposited and implanted films are shown in Fig. 3. These spectra are typical of disordered carbon and consist of two components usually referred to as bands D (the shoulder at lower energy) and G (the main spectral feature), respectively. The ratio between the intensities of the D and G bands, ( $I_D/I_G$ ), is an indication of the degree of disorder in an amorphous carbon film. Higher values of this ratio correspond to an increase of the disorder. As is clear from Fig. 3,  $I_D/I_G$  increases with the ion fluence. The position of the G band shifts to higher frequencies and is accompanied by a slight reduction of its width, indicating a progressive graphitization of the near-surface

layer under ion bombardment. An accurate description of the Raman experiments and data analysis was published before by our group<sup>[8-10]</sup>. The spectrum of the sample implanted with  $2 \times 10^{16}$  N/cm<sup>2</sup> is not shown in the figure because it is identical to that obtained for the as-deposited film.

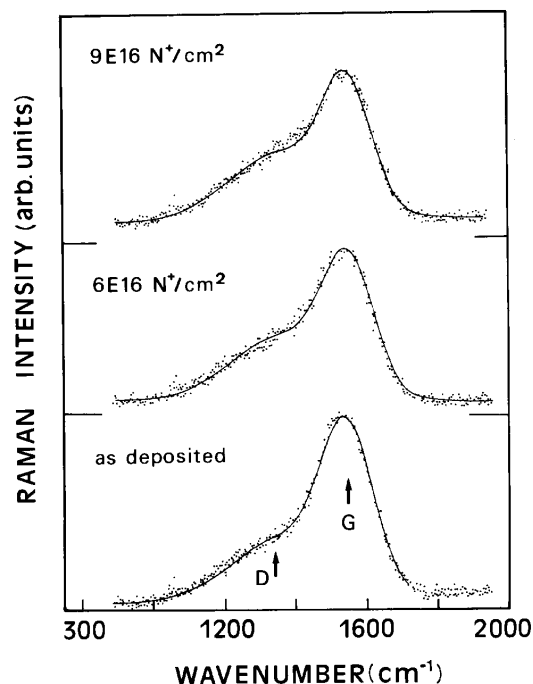


Figure 3. Raman spectra for as-deposited and implanted a-C:H films. The solid lines are the fitted spectra, using a simple model in order to reproduce the data as a sum of two gaussian lines. The position of D and G bands are indicated by arrows.

#### IV. Discussion and Conclusions

The SIMS results are in good agreement with TRIM-90 predictions and with previous measurements using nuclear techniques<sup>[9,18]</sup>. The experimental values for  $R_p$  and  $\Delta R_p$  agree with the theoretical simulation, which give us confidence to use TRIM-90 results for a first interpretation of PAS data. However, we need to be careful with the quantitative predictions of TRIM, because there are some experimentally unknown parameters for amorphous carbon films, as for example, the displacement energy, which have strong influence on the depth distribution of the vacancies. An additional limitation of the TRIM-90 code is that it do not take into account any dynamic effect as, for example, defects annihilation under ion bombardment or vacancy cluster formation.

In Fig. 4 we present TRIM simulations for a 70-keV N implantation into a-C:H films. This figure shows the deposited energy by elastic and inelastic collisions. The theoretical  $R_p$  position is also indicated. To compare the amount of lattice damage produced by different ions and energies, the number of displacements per atoms ( $DPA$ ) is frequently used<sup>[6]</sup>. A unit of  $1DPA$  means that, on average, every atom in the affected volume has been displaced once from its equilibrium lattice. The dependence of  $DPA$  with depth  $x$ , is given by<sup>[6]</sup>:

$$DPA(x) = 0.8\nu_{el}(E, x)\phi/(2E_dN) \quad (2)$$

where  $\nu_{el}(E, x)$  is the deposited energy by elastic collisions,  $N$  the atomic density (atom/cm<sup>3</sup>),  $\phi$  the ion fluence and  $E_d$  the displacement energy (20 eV, arbitrarily chosen in the present work). Therewith, the curve  $\nu_{el}(E, x)$  shown in Fig. 4 is proportional to  $DPA$ . From equation (2), when we increase the ion fluence,  $DPA$  also increases.

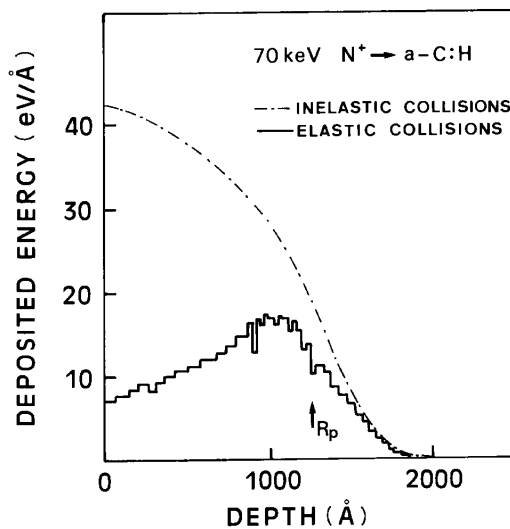


Figure 4. Monte-Carlo simulation results (TRIM-90) for the energy deposited by elastic and inelastic collisions in N-implanted a-C:H film, as a function of the depth. The theoretical  $R_p$  position is indicated by an arrow.

The depth profile for the  $S$  parameter obtained for the films implanted with  $2 \times 10^{16}$  N/cm<sup>2</sup> nicely follows the trend described by  $\nu_{el}(E, x)$ . In fact, we expect that the ionization profile does not play an important role concerning point defect formation. At this low fluence, we did not observe either hydrogen loss (SIMS results) or structural modifications (Raman results). Then, we can conclude that, in this case, positron annihilation

results directly reflect the depth distribution of point defects created by nitrogen irradiation.

The observed reduction of  $S$  for higher ion fluences seems to contradict the above conclusion. As is clear from equation (2), if we exclude the possibility of any type of dynamic annealing of defects under irradiation, an increase of fluence can be followed by an increase of the density of point defects, and so, an increase of  $S$  value. This behavior was observed, for example, in hydrogen implanted Si crystals<sup>[17]</sup>. However, in amorphous carbon, the structural modifications play an important role.

A multitechnique approach to determine the structural modifications induced in implanted a-C:H films<sup>[8-10]</sup> has clearly shown that both the degree of disorder and the number, or the size, of graphitic domains increase upon increasing of the ion fluence. Auger electron spectroscopy and Raman scattering experiments indicate the graphitization of a near-surface layer,  $R_p + \Delta R_p$  thick, under ion bombardment. We correlated these modifications with the total deposited energy by the atomic collisions<sup>[8,9]</sup>, which is nearly constant throughout all the modified layer. The hydrogen depletion that occurs only for fluences higher than  $2 \times 10^{16}$  N/cm<sup>2</sup>, also increases with the ion fluence. Raman results, presented in Fig. 3 and SIMS profiles, presented in Fig. 1, illustrate these two points.

An interpretation of the  $S$  parameter measured in the regime of fluences higher than  $2 \times 10^{16}$  N/cm<sup>2</sup> necessarily needs to take into account both structural and compositional modifications. The increase of the number of displacements induced by the incident particles and the observed hydrogen loss should correspond to an increase of the density of open-volumes, increasing the  $S$  parameter. Otherwise, the structural modifications, ion induced graphitization, reduces  $S$ . It was observed both in annealed a-C:H films<sup>[19]</sup> and on diamondlike nanocomposite films deposited under several deposition conditions<sup>[15]</sup>. In this last case, Raman results indicate that films with graphitic-like behavior corresponds to lower values of the  $S$  parameter<sup>[19]</sup>. It indicates that PAS results reflects, in a very complex way, the structural modifications in the disordered carbon network. In the case of our implanted samples, despite the degree of modifications induced by ion implantation is significantly lower than that introduced by annealing

in similar films<sup>[20]</sup>, a reduction on  $S$  was also observed. So, we can explain the shape of the  $S$  depth profiles, all nearly parallel to those obtained for the lowest fluence, as an indication of a memory of the lattice damage distribution, the value of  $S$  parameter depending on the degree of ion induced graphitization. However, much more work is needed in order to transform the PAS technique in a quantitative tool for the characterization of the structural modifications and the open-volumes distribution in amorphous carbon materials.

In summary, the  $S$  parameter follows the lattice damage depth profile predicted by the Monte Carlo simulation for nitrogen fluences of  $2 \times 10^{16}$  N/cm<sup>2</sup>. For higher fluences, we observed a reduction in the measured value of  $S$ . This result can be interpreted as being due to both structural (increase of disorder and of the number of graphitic domains) and compositional (hydrogen loss) modifications induced in the carbon film and by the point defects generated during the ion stopping process.

### Acknowledgements

This work is supported in part by Brazilian agencies MCT, CNPq, FINEP, and PADCT-Novos Materiais.

### References

1. J. Robertson, Prog. Solid State Chem. **21**, 199 (1991).
2. J.C. Angus, Y. Wang and R.W. Hofman, in *New Diamond Science and Technology*, edited by R. Messier, J.T. Glass, J.E. Butler and R. Roy (Materials Research Society, Pittsburgh, 1991)p. 11.
3. O. Amir and R. Kalish, J. Appl. Phys. **70**, 4958 (1991).
4. D. F. Franceschini, C. A. Achete and F. L. Freire Jr., Appl. Phys. Lett. **60**, 3229 (1992).
5. O. Amir and R. Kalish, Diamond Relat. Mater. **1**, 364 (1992).
6. G. Compagnini and L. Calcagno, Mater. Sci. Eng. R **13**, 193 (1994).
7. G. L. Doll, I. P. Heremans, T. A. Perry and J. V. Mantese, J. Mater. Res. **9**, 85 (1995).
8. F. L. Freire Jr., C. A. Achete, D. F. Franceschini, C. Gatts and G. Mariotto, Nucl. Instr. Meth B **80/81**, 1464 (1993).
9. F.L. Freire Jr., C. A. Achete, D. F. Franceschini and G. Mariotto, Appl. Phys. **A59**, 667 (1994).
10. F. L. Freire Jr., C. A. Achete and G. Mariotto, Nucl. Instr. Meth **B99**, 606 (1995).
11. P. J. Schultz and K. G. Lynn, Rev. Mod. Phys. **60**, 701 (1988).
12. G. Kogel, D. Schödlbauer, W. Triftshäuser and J. Winter, Phys. Rev. Lett. **60**, 1550 (1988).
13. F. Rossi, B. André, A. van Veen, P. E. Mijnaerends, H. Schut, M. P. Delplancke, W. Gissler, J. Haupt, G. Lucazeau and L. Abello, J. Appl. Phys. **75**, 3121 (1994).
14. F. L. Freire Jr., C. A. Achete, R. S. Brusa, G. Mariotto, X. T. Teng and A. Zecca, Solid State Comm. **91**, 965 (1994).
15. P. Asoka-Kumar, B. F. Dorfinan, M. G. Abraizov, D. Yan and F. H. Pollak, J. Vac. Sci. Technol. **A13**, 1044 (1995).
16. J. F. Ziegler, J. P. Biersack, U. Littmark, *The stopping and range of ion in solids*, Vol. 1, (Pergamon Press, New York, 1985).
17. R. S. Brusa, M. Duarte-Maia, A. Zecca, C. Nobili, G. Otaviani, R. Tonini and Dupasquier, Phys. Rev. B **49**, 7271 (1994).
18. F. L. Freire Jr., D. F. Franceschini and C. A. Achete, Nucl. Instr. Meth B **85**, 268 (1994).
19. F. L. Freire Jr., D. F. Franceschini, C. A. Achete, R. S. Brusa, G. Karwasz, G. Mariotto and R. Canteri (unpublished).
20. F. L. Freire Jr., C. A. Achete, G. Mariotto and R. Canteri, J. Vac. Sci. Technol. A, **12**, 3048 (1994).